Integrated IVUS-OCT for Real-Time Imaging of Coronary Atherosclerosis

Jiawen Li, MS, **Xiang Li, PhD**[*], **Dilbahar Mohar, MD**, **Aidan Raney, MD**, **Joseph Jing, MS**, **Jun Zhang, PhD**, **Abbey Johnston, MD**, **Shanshan Liang, MS**, **Teng Ma, BS**, **K. Kirk Shung, PhD**, **Sari Mahon, PhD**, **Matthew Brenner, MD**, **Jagat Narula, MD**, **Qifa Zhou, PhD**, **Pranav M. Patel, MD**, and **Zhongping Chen, PhD**

Department of Biomedical Engineering (J.L., J.J., J.Z., S.L. and Z.C.), Division of Cardiology (D.M., A.R. and P.M.P.), Division of Pulmonary and Critical Care (M.B.), Department of Pathology and Laboratory Medicine (A.J.), Beckman Laser Institute (J.L., J.J., J.Z., S.L., S.M., M.B. and Z.C.), The Edwards Lifesciences Center for Advanced Cardiovascular Technology (J.L., P.M.P. and Z.C.), University of California, Irvine, Irvine, CA, NIH Ultrasonic Transducer Resource Center (X.L., T.M., K.K.S. and Q.Z.), University of Southern California, Los Angeles, CA, and Mount Sinai Medical Center, New York, NY (J.N.)

Abstract

Objective—Combined use of optical coherence tomography (OCT) and intravascular ultrasound (IVUS) is a potential method for accurate assessment of plaques characteristics and vulnerability. The aim of this study is to develop and evaluate the feasibility of a fully integrated intracoronary OCT-IVUS imaging technique to visualize plaques in living animals.

Background—*In vivo* imaging of plaques by an integrated OCT-IVUS system has not been reported.

Methods—Simultaneous real-time OCT-IVUS imaging is performed using an integrated OCT-IVUS system and a single fully-integrated catheter with a 3.6F outer-diameter same as a commercial IVUS catheter.

Results—To verify *in vivo* imaging capability of this technique, five atherosclerotic-model rabbits and a swine were imaged. Images were obtained in these animals without complications. Linear regression shows a high correlation between rabbit plaque sizes determined from histology and OCT/IVUS estimated plaque sizes (R^2=0.955, P<0.001 between OCT and histology; R^2=0.970, P<0.001 between IVUS and histology). Classification of plaque types and quantitative analysis of plaque sizes were performed *in vitro* using cadaver coronary segments (n=14).

Conclusions—For the first time, this study shows that an integrated intracoronary OCT-IVUS system is feasible and safe to use *in vivo* to detect atherosclerotic plaques. This technique provides high resolution and deep penetration capability simultaneously which can facilitate a more

Correspondence to: Zhongping Chen, Ph.D. 1002 Health Sciences Road East Beckman Laser Institute University of California, Irvine Irvine, CA 92612 Phone: 949-824-1247 Fax: 949-824-8413 z2chen@uci.edu Pranav M. Patel, MD, FACC 101 City Drive South City Tower, Suite 400, Orange, CA 92868 Phone: (714) 456-6699 Fax: (714) 456-8895 pranavp@uci.edu Qifa Zhou, Ph.D. 1042 Downey Way, University Park NIH Ultrasonic Transducer Resource Center University of Southern California Los Angeles, CA 90089 Phone: 213-740-9475 Fax: 213-821 3897 qifazhou@usc.edu.
[*]co-first author

powerful tool to explore the development of plaques and may lead to a more accurate assessment of vulnerable plaques in patients.

Keywords

Vulnerable plaque; intravascular ultrasound; optical coherence tomography; intracoronary imaging

---

Accurate assessment of atherosclerotic plaque characteristics and the subsequent tailoring of optimal therapy holds great promise for preventing acute coronary syndrome (ACS) and life-threatening sequelae (1). Combined use of optical coherence tomography (OCT) and intravascular ultrasound (IVUS) was proposed as a potential method for accurate assessment of plaque characteristics and vulnerability (2,3). However, significant challenges remain in trying to adapt an integrated OCT-IVUS system for clinical applications. This letter reports a fully integrated intracoronary OCT-IVUS imaging technique to visualize atherosclerotic plaque in living animals and human coronary arteries from cadavers with high resolution and deep penetration capability simultaneously.

First, we created lesions, similar to human atherosclerotic plaques, in male New Zealand white rabbits by feeding them a high cholesterol diet and de-endothelization procedures (4). We proceeded with imaging plaques in rabbit aortas using the OCT-IVUS system with a 3.4 French integrated catheter (5) and a 10 ml Omnipaque (iohexol, 350mI/mL) flushing into the artery at ~3 ml/s for blood clearance. A total of 10 volumetric data sets were obtained from 5 rabbits. Ten 2-20 mm long aorta segments were imaged at 5mm/s pull-back speed. A representative OCTIVUS image pair and corresponding histology of a rabbit abdominal aorta with a *thick* cap fibroatheroma is shown in Fig. 1 row I. IVUS enables the visualization of the layer structure of the artery wall. Intimal thickening and a low density acoustic signal region (denoted by the arrow in Fig. 1 Ia) demonstrate plaque in the IVUS image. However, this image also illustrates the inability of IVUS to determinate the plaque type and the plaque cap boundary. At the same site in the OCT image (Fig. 1 Ib), a homogenous-boundary and weak-signal region under a high-signal region indicates that this plaque is a necrotic/lipid plaque with an overlying fibrous cap. Also, the minimum thickness of the cap can be easily measured to be ~200 μm by OCT, which is indicative of a thick cap fibroatheroma. The classification of plaque type is validated by the corresponding histology photo (Fig. 1 Ic) which shows loose necrotic material. This area is covered by smooth muscle and fibrous proliferations at the luminal surface, which is consistent with a fibrous cap. All IVUS-OCT images of rabbit aortas were matched with histology for accuracy correlation. Linear regression showed a high correlation between plaque circumference percentage (PCP, defined as the circumference of lumen where there is plaque divided by the entire lumen circumference) determined from histology and the estimated PCP of OCT and IVUS (R^2=0.955, P<0.001 between OCT and histology; R^2=0.970, P< 0.001 between IVUS and histology).

Second, a female Yorkshire white swine was imaged by conventional femoral access and angiography guidance under the same flushing procedure as the rabbits to test the feasiblity of translating this technology for clinical applications (Figs. 1 row II). In the IVUS image (Fig. 1 IIa), the three-layer structure of the swine artery (wall thickness ~0.4 mm) is barely visualized with an IVUS resolution of 60 μm. In Fig. 1 IIb, the OCT image differentiates the three structural layers of the artery wall.

Last, we collected 14 cadaver coronary arteries from 6 patients who died of complications from ACS or were diagnosed with atherosclerotic heart disease. Representative OCT-IVUS image pairs of a fibrous plaque, calcified plaque and lipid plaque from different cadavers are

shown in Fig. 1 row III, IV and V respectively. An acoustic shadow in Fig. 1 IVa shows the location of a calcified plaque. However, it is difficult to classify the plaque morphology in Fig. 1 IIIa and Fig. 1 Va using IVUS imaging because of intrinsically limited resolution and low soft tissue contrast. The OCT imaging is able to classify plaque morphology by optical scattering contrast of different tissue types (see Figure 1 legend). However, with limited penetration depth, the OCT image cannot provide a clear visualization of the media and adventitia layer at this intima-thickening coronary segment. These results clearly demonstrate the complementary nature of OCT and IVUS imaging. A total of 28 OCT-IVUS image pairs, obtained from 14 plaque samples (two pairs from each sample, pull-back and repull-back), were analyzed for quantitative validation of the technique's accuracy and reproducibility. Linear regression showed a high accuracy (R^2=0.911, P<0.001 for OCT-histology; R^2=0.923, P<0.001 for IVUS-histology) and high reproducibility (R^2=0.937, P<0.001 for OCT and R^2=0.971, P<0.001 for IVUS) of PCP measurements.

Our fully integrated *in vivo* imaging system has high resolution to identify the thin cap and deep penetration to visualize the necrotic core simultaneously. Such a device may lead to a more accurate assessment of vulnerable plaques and especially thin-cap fibroatheroma (TCFA). Moreover, most of the current understanding about ACS has been achieved by static histopathology research. This novel *in vivo* integrated OCT-IVUS imaging technique is anticipated to improve our understanding of the process of this disease through longitudinal *in vivo* studies.

Acknowledgments

Abbreviation list

ACS	acute coronary syndrome
OCT	optical coherence tomography
IVUS	intravascular ultrasound
TCFA	thin-cap fibroatheroma
EEL	external elastic lamina
H&E	hematoxylin and eosin
CD 68	cluster of differentiation 68
PCP	plaque circumference percentage

Reference

1. Fleg JL, Stone GW, Fayad ZA, et al. Detection of high-risk atherosclerotic plaque: report of the NHLBI Working Group on current status and future directions. JACC Cardiovasc Imaging. 2012; 5:941–55. [PubMed: 22974808]

2. Sawada T, Shite J, Garcia-Garcia HM, et al. Feasibility of combined use of intravascular ultrasound radiofrequency data analysis and optical coherence tomography for detecting thin-cap fibroatheroma. European Heart Journal. 2008; 29:1136–1146. [PubMed: 18397871]

3. Puri R, Worthley MI, Nicholls SJ. intravascular imaging of vulnerable coronary plaque: current and future concepts. Nature reviews. 2011; 8:131–139.

4. Kolodgie FD, Petrov A, Virmani R, et al. Targeting of Apoptotic Macrophages and Experimental Atheroma With Radiolabeled Annexin V. Circulation. 2003; 108:3134–3139. [PubMed: 14676140]

5. Yin J, Li X, Jing J, et al. Novel combined miniature optical coherence tomography ultrasound probe for in vivo intravascular imaging. Journal of biomedical optics. 2011; 16:060505. [PubMed: 21721799]

Condensed abstract

Atherosclerotic plaques are the usual cause of coronary artery disease. For the first time, our study shows that an integrated OCT-IVUS system is feasible and safe to use *in vivo* to detect atherosclerotic plaques. This technique provides high resolution and deep penetration capability simultaneously which facilitates a more powerful tool to explore the development of plaques and may lead to a more accurate assessment of vulnerable plaques in patients.
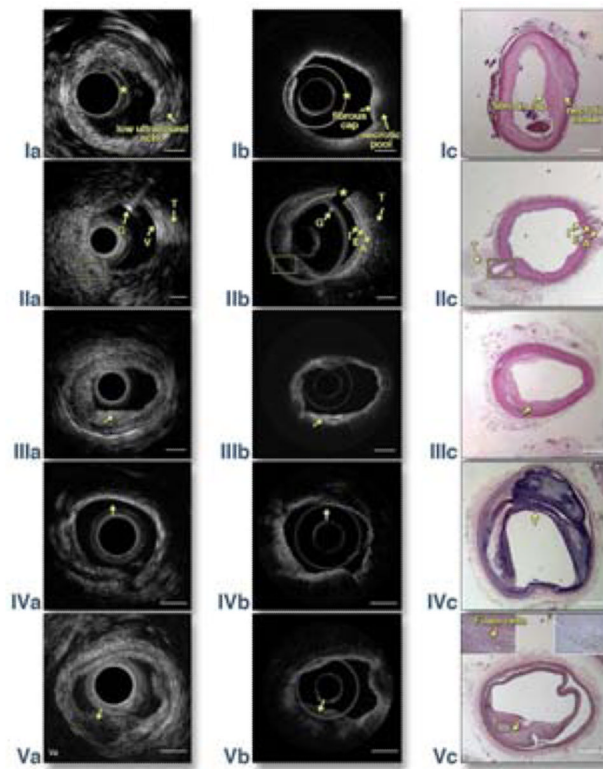
Figure 1. Top row: *In vivo* **imaging of rabbit abdominal aorta with OCT-IVUS system**
IVUS (Ia) and OCT (Ib) cross-sectional images of atherosclerosis microstructure in a rabbit; (Ic) corresponding H&E histology. Artifact circles in IVUS images, * in (Ia), are due to the ultrasound pulse ring down effect and the reflection of the catheter sheath. Artifact circle in OCT image, * in (Ib), is caused by the high back reflection from the interface between the prism and GRIN lens. The shape of this artery changed between *in vivo* imaging (Ia) and histology (Ic) due to the reduced intra-lumen pressure after this artery was harvested.
Second row: An OCT-IVUS image pair obtained in a normal swine coronary artery *in vivo*. (IIa) OCT image, (IIb) IVUS image, and (IIc) corresponding H&E histology. Guidewire artifact is denoted by* in (IIa); G: guide wire; T: tissue; V: vessel; I: intima; E: EEL; A: adventitia. Yellow boxes denote LAD branch. From the center of the OCT image, there is a high-signal thin band corresponding to the intima, followed by a high-signal strip corresponding to the external elastic lamina (EEL), and finally a low-signal area corresponding to the adventitia.
Bottom three rows: Imaging of a coronary artery with a fibrous plaque (third row), calcified plaque (fourth row) and lipid plaque (bottom row). (IIIa)(IVa)(Va) IVUS images, (IIIb)(IVb)(Vb) OCT images, and (IIIc)(IVc)(Vc) corresponding histology images. Insets in (Vc) are highly magnified images of the histology slides: left inset, stained with H&E; right inset, stained with CD68. Arrows denote the location of plaques. Plaque types can be classified based on optical scattering contrast of different tissue types: 1) signal-rich regions from 5 o' clock to 7 o'clock in (IIIb) indicate a fibrous plaque; 2) a sharp-boundary, signal-poor region from 11 o' clock to 4 o'clock in (IVb) indicates a calcified plaque; 3) a diffusive-boundary, signal-poor region from 5 o' clock to 7 o'clock in (Vb) indicate a lipid plaque. The histology results confirm the classification of plaque types by the OCT and IVUS images: the dense, compact eosinophilic fibers (in IIIc) represent increased amounts of collagen seen in a fibrous plaque. In (IVc), the residual calcium can be seen as numerous irregular refractile purple crystals. In (Vc), foam cells and dark brown staining in the CD 68 stain slide verify

that this is a lipid plaque. Note for (Vc): as this excised tissue is older (~10 months postmortem), the degraded nuclear material did not stain well with hematoxylin. Although the tissue is predominantly pink in color, the structure and architecture are preserved. Scale bar: 1mm.